Very Dense Seismic Array Observations in Furukawa District, Japan

Hiroyuki Goto[1], Hitoshi Morikawa[2], Masayuki Inatani[1], Yumiko Ogura[2], Satoshi Tokue[2], Xin-Rui Zhang[2], Masahiro Iwasaki[3], Masayuki Araki[4], Sumio Sawada[1], and Aspasia Zerva[5]

[1]Kyoto University, Japan

[2]Tokyo Institute of Technology, Japan

[3]Government of Osaki City, Japan

[4]aLab Co.Ltd, Japan

[5]Drexel University, USA

1 Introduction

On March 11, 2011, the off the Pacific Coast of Tohoku Earthquake (M_W9.0) hit the eastern part of Japan's mainland, and killed more than ten thousand peaple mainly due to great tsunami in the immediate on-shore region. On

the other hand, strong ground motions during the earthquake were observed in almost the whole region of Japan by K-NET, KiK-net organized by National Research Institute for Earth Science and Disaster Prevention (NIED), and the other seismometer networks. At least 17 of the K-NET and KiK-net stations observed over 980 cm/s^2 of PGA in horizontal components, and two stations observed over 6.5 of high seismic intensity on the Japan Meteorological Agency (JMA) scale. However, damage in areas due to ground motion do not correspond to either the large PGA or the high seismic intensity (e.g. Motosaka, 2012; Goto and Morikawa, 2012).

We focus on the Furukawa District of Osaki City, where severe residential damages occurred downtown. Ground motion records in the downtown area are available at two stations, MYG006 (K-NET) and JMA Furukawa (JMA). The damage level was different between the areas within several hundred meters from the MYG006 and JMA Furukawa stations, which are about 1 km away from each other. The severe damages were concentrated within the area approximately 1x1 km^2 including the JMA station. This implies that the ground motion characteristics were not uniform in sub-kilometer scale, and the existing two stations are not enough to clarify the damage distribution.

In aftermath of the earthquake, we distributed dozens of low-cost seismometers, namely ITK sensor, around the area about 3x2 km^2 in the Furukawa district. The observed data are sent to the remote server through internet connection in real time. The seismometers were installed beside the volunteers' houses. The volunteers can access the interactive information service, namely on-line viewer system. In this article, we describe the seismic array observation in detail, and analyze the ground motion data of minor earthquakes.

2 Ground Motions during the 2011 Earthquake in the Furukawa District

During the Off the Pacific Coast of Tohoku Earthquake, severe structural damages occurred in the Furukawa District of Osaki City, which is located at approximately 35 km north of Sendai City (Figure 1). The Furukawa station of JR Tohoku Shinkansen (Bullet Train) and JR Riku-u-tosen are located in the center of the district. There are four seismic stations in the area, K-NET MYG006, JMA Furukawa, Furukawa Gas, and NILIM (National Institute for Land and Infrastructure Management) Furukawa. However, the

Furukawa Gas station, unfortunately, did not record the main shock (Goto *et al.*, 2012). The K-NET MYG006, JMA Furukawa, and NILIM Furukawa stations recorded PGAs of 583 cm/s^2, 568 cm/s^2, and 483 cm/s^2, respectively, and the corresponding seismic intensities on the Japan Meteorological Agency (JMA) scale are 6.1, 6.2, and 6.1.

The Furukawa district is located on Osaki plain, which is covered by Holocene sediments (Geological Survey of Japan, AIST, 2010), and the terrain is almost flat with elavations from 17 to 21 m. The soil property of 20 m in depth is available at K-NET MYG006, as shown in Figure 2. The soft surface layer, consisting of silt, sand, and organic soil, with approximately 10 of standard penetration test (SPT) N-values and 130 m/s of S-wave velocities overlays relatively hard gravels with over 50 of SPT N-values and 400 m/s of S-wave velocity.

Damage distribution based on the reconnaissance immediately after the main shock is reported in Goto and Morikawa (2012). Figure 3 shows the details of the damage distribution and the location of the seismic stations, K-NET MYG006 and JMA Furukawa. The Furukawa Gas station is located approximately 1 km west of the area, and the NILIM Furukawa station is located approximately 2 km east of the area. Damages due to the liquefaction

were observed in the western area of the JR Furukawa station, and due to the ground motion in the area neighboring the liquefaction area.

The damage level was different between the areas within several hundred meters from the K-NET MYG006 and JMA Furukawa stations, which are approximately 1 km away from each other. The severe damages were concentrated within the area approximately 1x1 km^2 including the JMA station. The reasons are not yet clearly understood, but may be attributed, e.g., to different structure types, differences in the ground motions, etc. Figure 4 shows the velocity response spectra (for damping h=0.05) of the two horizontal components during the main shock at the K-NET MYG006 and JMA Furukawa stations, which are compared to the corresponding spectra of the JR Takatori record during 1995 Kobe earthquake. The spectra observed in the Furukawa district show similar shapes, especially in the period range of 1-2s, to ones of the Kobe earthquake, which has caused destructive damage of structure: this is not the case for the spectra of the MYG006 record. It is noted that the JMA Furukawa station is closer to the severely damaged area than the MYG006 one. This suggests that the power of the ground motions around 1s plays an important role in the damage to structures, and that the spatial variation of the ground motions may be critical for the damage.

3 Installation of Very Dense Seismic Array

In order to quantify the spatial variation of the ground motion characteristics, we developed a very dense seismic array in the Furukawa district.

We installed low-cost seismometers, namely ITK sensors, to form the array illustrated in Fig.5. The sensors require AC power supply and internet connection for data streaming. The original system of the ITK sensors uses the NTP (network time protocol) to synchronize the inner clock. NTP supports enough accuracy in a closed network system, however, it does not suffice in a case where packets of NTP pass through a gateway or router. To insure the time accuracy, we modified the ITK system to adjust to the clock signal from GPS (global positioning system).

We requested the cooperation of the residents of the Furukawa district through the Osaki City office. We oddered the volunteers three terms in order to participate to the project: 1) an appropriate place to allocate AC power supply, 2) free usage of the internet connection, and 3) installing the sensor on a concrete slab using gypsum. The number of volunteers for setting up the sensors gradually increased. As a result, we have installed 23 sensors by the end of February 2012. All sensors are located inside a 3x2 km^2 area in the Furukawa district, as shown in Fig.5. Some sensors are set very closely to

one another such as F06 and F07. They are located inside one residence: one is set on original ground and the other on improved ground. F17 is located at approximately a 50 m distance from the K-NET MYG006 station.

Seismic array observations have been extensively performed in the past. For example, the Yokohama City high-concentration seismograph network (e.g. Abe *et al.*, 1997) organized by the Yokohama City office covers approximately 400 km^2 by 150 stations, i.e., a 2.5 km^2 area covered by a sensor. The SUPREME system (e.g. Shimizu *et al.*, 2001) organized by Tokyo Gas covers approximately 3,100 km^2 by 3,700 SI sensors, i.e., a 0.8 km^2 area covered by a sensor. The San Jose seismic array (e.g. Hartzell *et al.*, 2003) covers approximately 5x6 km^2 by 52 sensors, i.e., a 0.6 km^2 area covered by a sensor. Our seismic array in the Furukawa district covers a 3x2 km^2 area with 23 sensors, i.e., a 0.25 km^2 area covered by a sensor. Although some off-line measurements without remote monitoring systems have been temporarily performed for the denser seismic array (e.g. Abrahamson *et al.*, 1991; Zerva and Stephenson, 2011), the array is the most dense network for strong ground motion observations with a modern remote monitoring system.

The sensor and a few components of the system are packed into one box, as shown in Figure 6. The inner components consist of the ITK sensor and an

equipment to connect the Ethernet LAN port of the sensor to a router located inside the residence. The system is selected from available connections by applying a Wifi convertor, PLC (Power Line Connection), or direct wired connection, depending on the situation. The observed data is sent to a remote server in sequence through the internet connection. Therefore, we can access the real-time data without retrieving the storage data at the actual sensor location.

To compensate the volunteers, we provide them with pseudo real-time information of the seismic intensity through an on-line viewer system, which is developed using the real-time data. The data is stored as one-minute binary files. Seismic intensities on the JMA scale corresponding to the one-minute data are calculated every one minute. The process is registered on the job scheduler in the main server. If more than half of the sensors observe an intensity over 0.0, the process turns on a flag of event trigger. At the same time, another process starts capturing the data from one-minute ahead of the trigger time until one-minutes past the time when more than half of the sensors observe less than 0.0 intensity. The process adds the detected event to a list file, the "event list file", and also the intensities of each sensor to another file, the "intensity list file", generated in JSON (JavaScript Object

Notation) format.

An on-line viewer system displays the distribution of seismic intensities on the Google Maps (Figure 7). Initially, it displays the distribution corresponding to the latest event, and users can rewind up to, at most, 100 events. The system asynchronously controls the display depending on user actions by using Google Maps API and the technique of Ajax. The system is accessible from Web browsers, and the volunteers can view the intensity distribution in the same way as with a usual Web site. When the sensors observe the event, the display is automatically updated within one minute.

4 Observed Data

The number of events detected by the above system was more than 100 by the middle of March 2012. Herein, we focus on two significant events observed in the array: #E1 on December 10th, 2011 and #E2 on January 1st, 2012. Figure 8 presents the accelerograms of the East-West component of the two events #E1 and #E2 on the left and right part, respectively. #E1 (Mw4.6) is the largest ground motion observed at the K-NET MYG006 station from the aftershocks of the Tohoku Earthquake after the installation of the array, and

#E2 (Mw6.8) is a deep-focus earthquake with the depth of 400 km. The accelerograms for #E1 contain much higher frequency components and shorter durations because an intrinsic damping Q and a seismic wave scattering less affects the high frequency components due to the shorter hypocenter distance such as 90 km for #E1 and 920 km for #E2. Data started being recorded at stations F01-F17 by December 10, 2011, and at stations F01-F19 by January 1, 2012: stations F08 and F10 for #E1 and stations F12 and F18 for #E2 did not record due to problems, as, e.g., a power outage, etc. Figure 8 suggests that the duration and general shape of the envelopes of the accelerograms are similar for each event, but the spatial variation of the ground motions is clearly obvious in the records. Figure 9 shows the Fourier amplitude of the accelerograms at the K-NET MYG006 station and stations F01-F17 during #E1 on the left part, and those at the K-NET MYG006 station and stations F01-F19 during #E2 on the right part. The figures clearly illustrate the differences in the sensor performance at low frequencies, which implies that the ITK sensors cannot reliably record ground motions for frequencies than 0.5 Hz.

Figure 10 presents the distribution of peak ground acceleration (PGA) of the horizontal components recorded by the seismic array, and the K-NET

MYG006 and the JMA Furukawa stations during events #E1 and #E2 events; it is noted that the data at the JMA Furukawa station have not been available for the latter event. PGAs for #E1 varied spatially in the ragnge of 18-38 cm/s^2; the smallest value is observed at station F16, and the largest value at station F13. For #E2, PGAs varied slightly less in the range of 17-30 cm/s^2; the smallest values are observed at the K-NET MYG006 station and station F15, and the largest value is observed at station F01.

In order to quantify the spatial variation of the motions, standard scores (SS) at each station are calculated, based on the following expression:

$$\mathrm{SS}_i = \frac{1}{N_i} \sum_{j \in S_i}^{N_i} \{10(x_{ij} - \mu_j)/\sigma_j + 50\}, \tag{1}$$

in which

$$\mu_j = \frac{1}{N_j} \sum_{i \in E_j}^{N_j} x_{ij} \tag{2}$$

$$\sigma_j{}^2 = \frac{1}{N_j} \sum_{i \in E_j}^{N_j} (x_{ij} - \mu_j)^2, \tag{3}$$

where x_{ij} is an observed value, such as PGA and PGV, at the ith station for the jth event. S_i and E_j are integers corresponding to the number of available records at the ith station and the jth event, respectively. N_i and N_j are the numbers of available records at the ith station and the jth event,

respectively. From the definition of Equation (1), SS_i is equal to 50 when the PGA or PGV values at site i is the average of all events, and SS_i is 40 or 60 when the PGA or PGV values are one standard deviation larger or smaller than the average value, respectively. The standard scores are calculated from the 23 stations belonging to the seismic array, and the K-NET MYG006 and JMA Furukawa stations. 23 earthquakes with PGA at the K-NET MYG006 station exceeding 5 cm/s^2 are selected from the records (Table 1).

Figure 11 shows the average of the standard scores (Eq.1) over the 23 earthquakes for the peak ground acceleration (PGA) and the peak ground velocity (PGV), which is evaluated from the integration of accelerograms band-passed in 0.5-10 Hz frequency range. In addition, Fig.11 presents the contour lines interpolated from the standard scores at the stations. It is observed that the PGA and PGV values around the central area are larger than those in the north-west area. This behavior may be correlated with the observed damage distributions (Figs.3 and 5).

Figure 12 shows the spectral ratio of the horizontal components of the motions at stations F01-23 with respect to the data at the K-NET MYG006 stations during the selected 23 earthquakes. The spectral ratios at each station are very similar for all examined earthquakes. This implies that

the spectrum ratio essentially corresponds to the relative site amplification, as site amplification is independent of the source-rupture mechanism and source-site distance. The dominant frequency range of the spectra also varies within 2-4 Hz depending on the sensor locations, and the spectral ratio decays to approximately 1 within 0.5-1.0 Hz. This may reflect variability in the shallow subsurface conditions underneath the array.

5 Conclusion

We deployed a very dense seismic array in the Furukawa district, where severe residential damages occurred downtown during the off the Pacific coast of Tohoku Earthquake. Sensors were distributed in intervals of a sub-kilometer scale, with a sensor covering an average area of approximately 0.25 km^2. Preliminary observations based on the array data are presented herein. The observed PGA and PGV values show significant spatial variability that may be correlated to the structural damage caused by the major 2011 event. We plan to continue the operation of the array for two years, and will analyze the observed data to gain insight into the spatial variation of the motions, physically and statistically. The results will be presented in the near future.

6 Acknowledgments

We thank the National Research Institute for Earth Science and Disaster Prevention for providing the records of the ground motions at the K-NET stations, the Japan Meteorological Agency, and the volunteers in the Furukawa district participating in this project.

References

Abe, S., Shinbo, Y., and Aoki, T., Observation results and studies of Yokohama city high-concentration seismograph network, *Proc. of 7th Institute of Social Safety Science*, 10-15, 1997 (in Japanese with English abstract).

Abrahamson, N., Schneider, J.F., and Stepp, J.C., Spatial coherency of shear waves from the Lotung, Taiwan large-scale seismic test, *Structural Safety*, **10**, 145-162, 1991.

Geological Survey of Japan, AIST, Seamless digital geological map of Japan 1:200,000. Feb. 1, 2010 version, *Research information Database DB084*, Geological Survey of Japan, National Institute of Advanced Industrial Science and Technology, 2010.

Goto, H., Morikawa, H., and Kuwata, Y., Estimation of ground motion at Furukawa gas during 2011 Tohoku-oki Earthquake, Proc. of 31st JSCE Earthquake Engineering Conference, 1-010, 1-7, 2011 (in Japanese with English abstract).

Goto, H. and Morikawa, H., Ground motion characteristics during the 2011 off the Pacific coast of Tohoku Earthquake, *Soils and Foundation*, submitted.

Hartzell, S., Carver, D., Williams, R.A., Harmsen, S., and Zerva, A., Site response, shallow shear-wave velocity, and wave propagation at the San Jose, California, dense seismic array, *Bull. Seism. Soc. Am.*, **93**, 443-464, 2003.

Motosaka, M., Lessons of the 2011 Great East Japan Earthquake focused on characteristics of ground motions and building damage, *Proc. International Symposium on Engineering Lessons Learned from the 2011 Great Easr Japan Earthquake*, 166-185, 2012.

Shimizu, Y., Koganemaru, K., Nakayama, W., Yamazaki, F., Development of super-dense real-time earthquake disaster mitigation system (SUPREME),

J. of Earthquake Engineering Research, JSCE, **26**, 1285-1288, 2001 (in Japanese).

Suzuki, W., Aoi, S., Sekiguchi, H. and Kunugi, T., Rupture process of the 2011 Tohoku-Oki mega-thrust earthquake (M9.0) inverted from strong-motion data, *Geophys. Res. Lett.*, **38**, L00G16, 2011.

Zerva, A. and Stephenson, W.R., Stochastic characteristics of seismic excitations at a non-uniform (rock and soil) site, *Soil Dynam. Earthquake Eng.*, **31**, 1261-1284, 2011.

Disaster Prevention Research Institute
Kyoto University
Gokasho, Uji, Kyoto 611-0011, Japan
goto@catfish.dpri.kyoto-u.ac.jp
(H.G.)

Table 1: Parameters of selected 23 earthquakes observed in the seismic array

	date	triger time (hh:dd JST)	latitude* (N deg)	longitude* (E deg)	depth* (km)	M_W**
	Nov. 2, 2011	10:43	39.006	141.775	63	4.3
	Nov. 24, 2011	04:24	37.330	141.613	45	6.1
	Nov. 29, 2011	03:53	38.628	141.930	48	4.4
	Nov. 30, 2011	21:55	38.423	141.998	63	3.8
	Dec. 2, 2011	09:50	38.186	141.776	56	4.7
	Dec. 3, 2011	13:16	38.885	141.980	50	4.6
	Dec. 5, 2011	04:20	38.179	141.768	56	4.3
(#E1)	Dec. 10, 2011	15:08	38.625	141.812	45	4.6
	Dec. 30, 2011	18:35	38.715	141.707	69	4.1
(#E2)	Jan. 1, 2012	14:29	31.428	138.567	397	6.8
	Jan. 9, 2012	07:13	39.341	142.064	48	5.2
	Jan. 12, 2012	12:21	36.968	141.304	33	5.5
	Jan. 12, 2012	14:37	38.377	142.622	28	5.3
	Jan. 18, 2012	17:55	38.619	141.910	48	4.3
	Jan. 23, 2012	07:52	38.673	141.883	56	4.0
	Jan. 26, 2012	05:43	38.176	141.693	51	5.2
	Jan. 28, 2012	09:23	40.153	142.427	36	5.6
	Feb. 12, 2012	04:56	38.725	142.187	42	4.6
	Feb. 16, 2012	14:09	38.546	142.075	42	4.3
	Feb. 24, 2012	04:28	39.009	142.312	58	4.7
	Feb. 28, 2012	01:30	38.536	141.821	50	4.6
	Mar. 8, 2012	12:23	38.530	141.819	50	4.8
	Mar. 14, 2012	18:09	40.775	145.228	64	7.0

* after JMA, ** after F-net by NIED

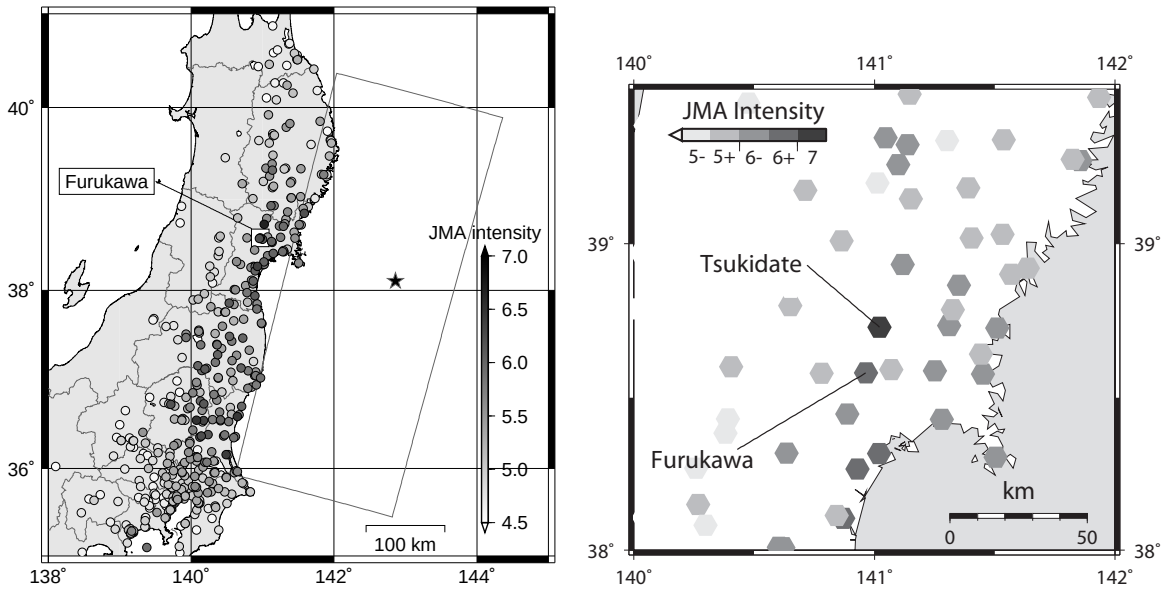

Figure 1: Left: The hypocenter and projected fault area (Suzuki *et al.*, 2011) during the 2011 Off the Pacific Coast of Tohoku Earthquake; the figure also illustrates the Furukawa district and the JMA intensity at the K-NET and KiK-net stations over the entire affected area during the main shock. Right: Zoom-in of the left part in the Furukawa district.

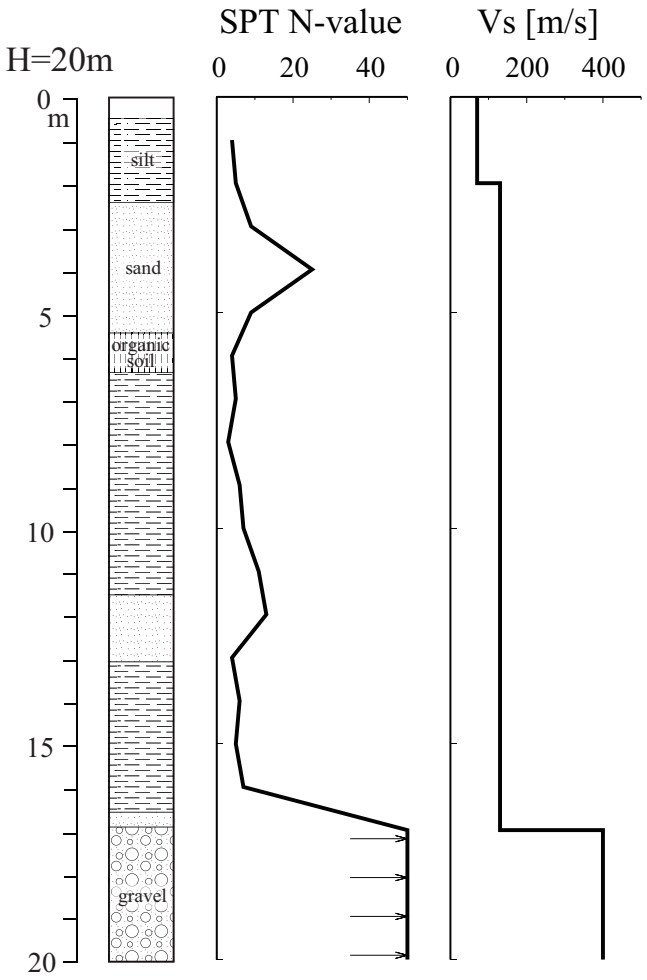

Figure 2: Soil property at K-NET MYG006 (after K-NET station informtation, NIED)

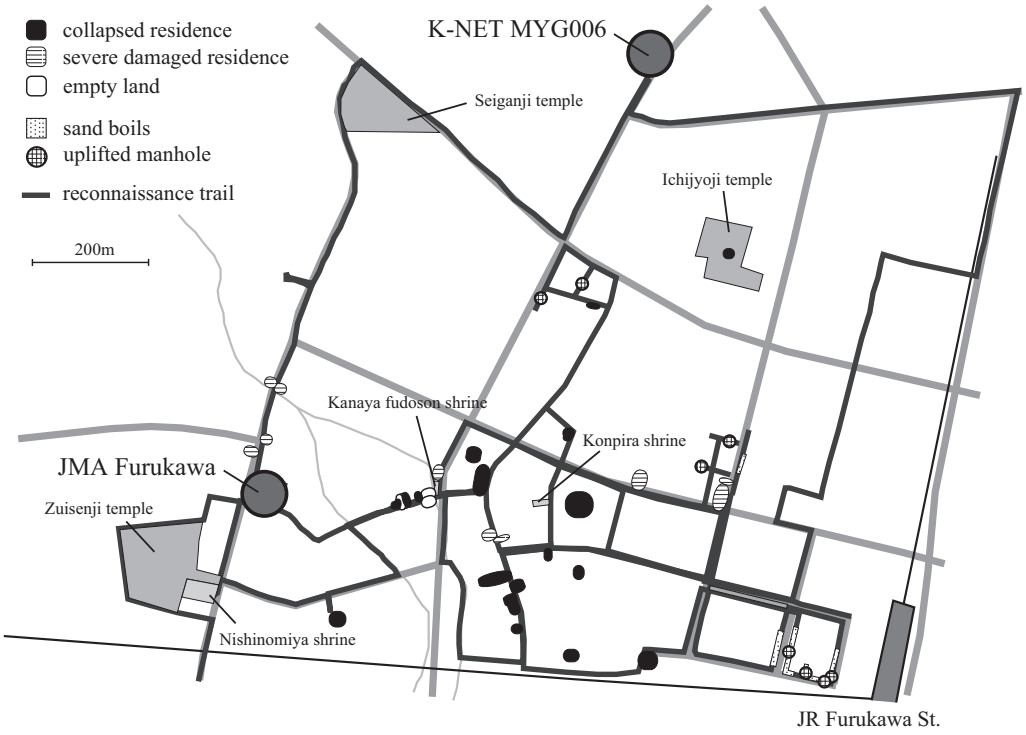

Figure 3: Location of the two seismic stations, K-NET MYG006 and JMA Furukawa, and illustration of significant damages in the Furukawa district.

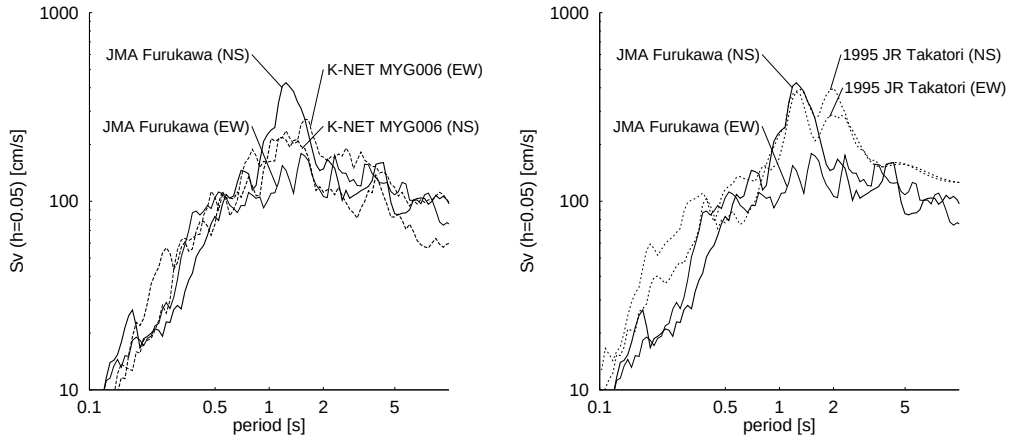

Figure 4: Comparison of the velocity response spectra (with damping h=0.05) of the two horizontal components recorded at the K-NET MYG006 and JMA Furukawa stations during the main shock, and those recorded at the JR Takatori station during the 1995 Kobe earthquake.

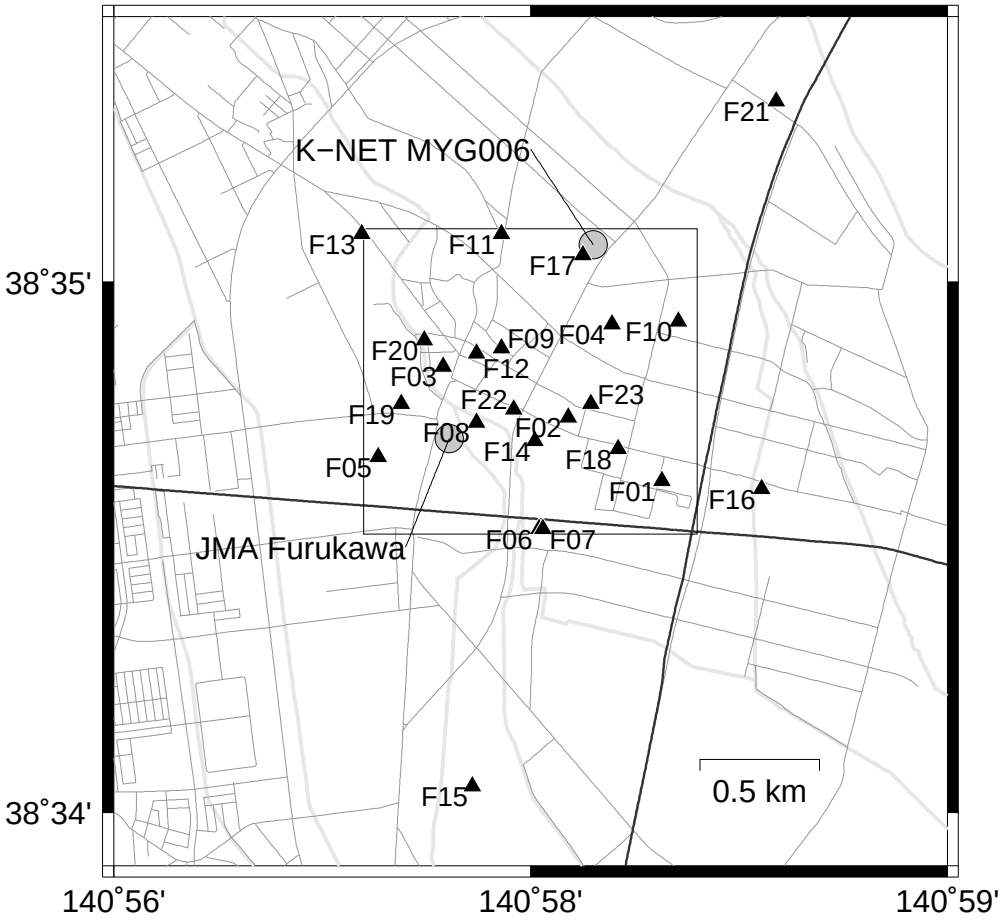

Figure 5: Sensor locations of the seismic array deployed in the Furukawa district. The square indicates the area corresponding to Fig.3 (Map data ©OpenStreetMap contributors, CC BY-SA)

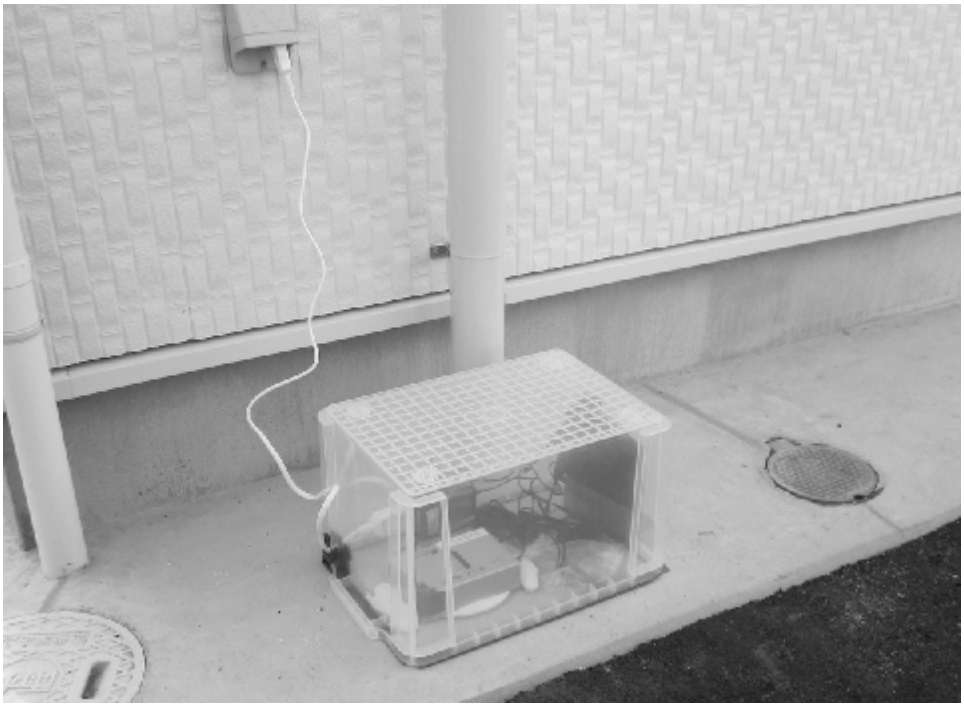

Figure 6: Illustration of the appearance of a representative system packed in a box. The photograph is taken at Station F07.

Figure 7: On-line viewer system displaying the distribution of seismic intensities at the array. The locations correspond to the station locations in Fig.3.

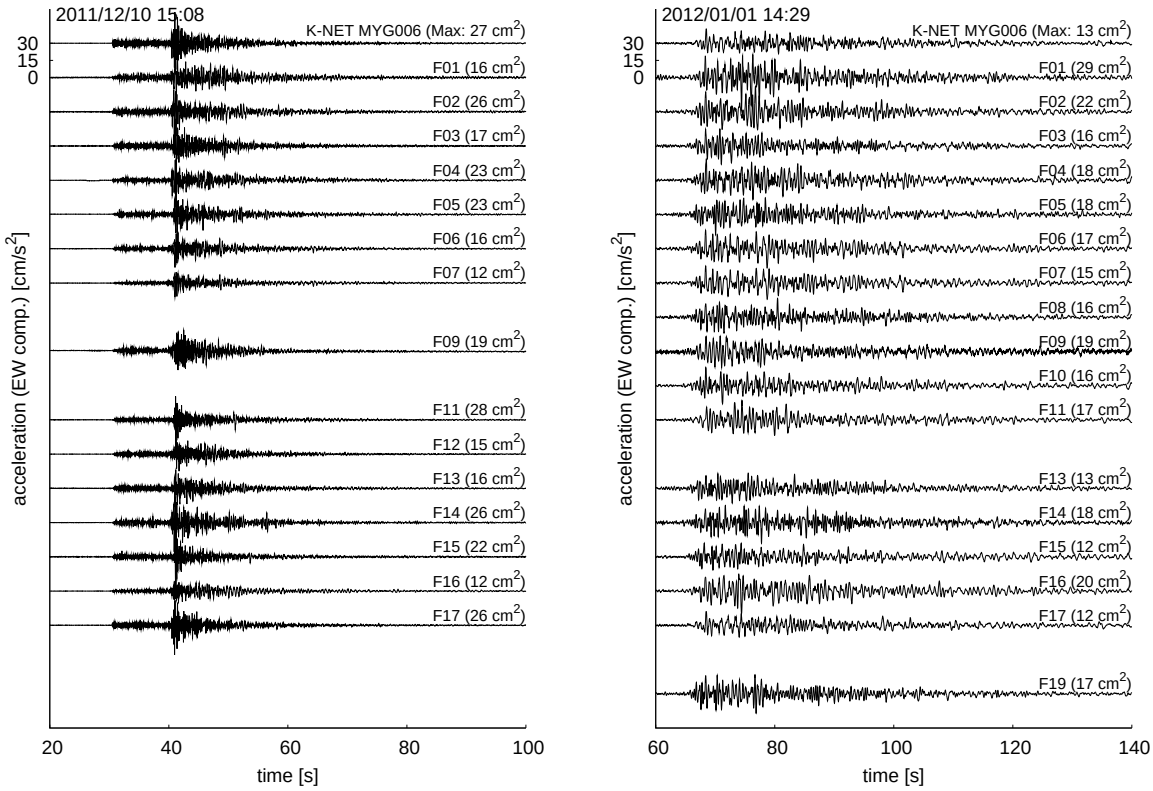

Figure 8: Accelerograms of the East-West component of #E1 recorded on December 10, 2011 (left part), and #E2 recorded on January 1, 2012 (right part).

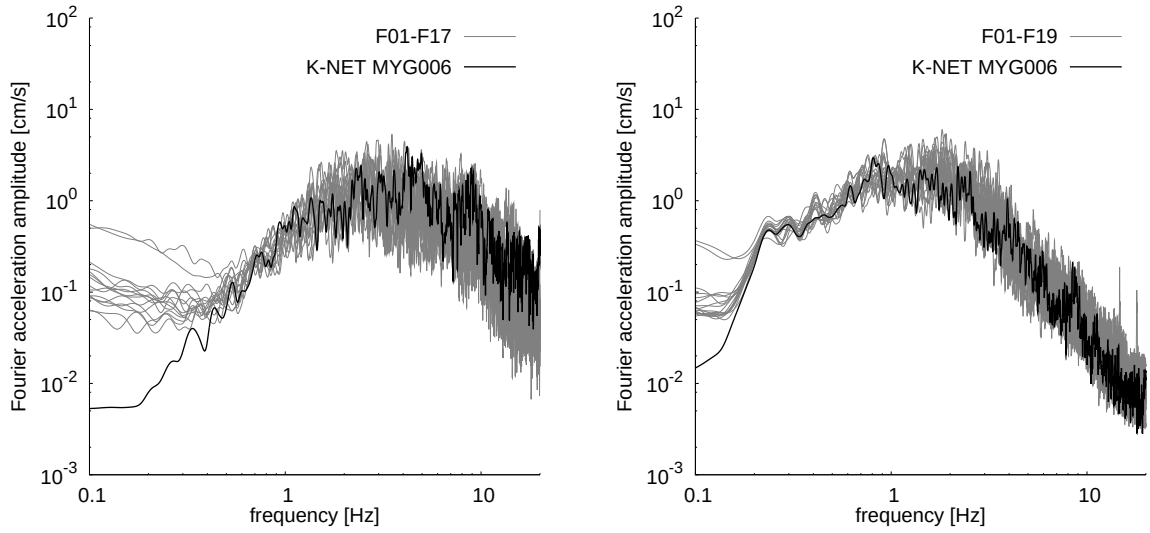

Figure 9: Fourier amplitudes of the accelerograms of the East-West component of #E1 recorded on December 10, 2011 (left part), and #E2 recorded on January 1, 2012 (right part).

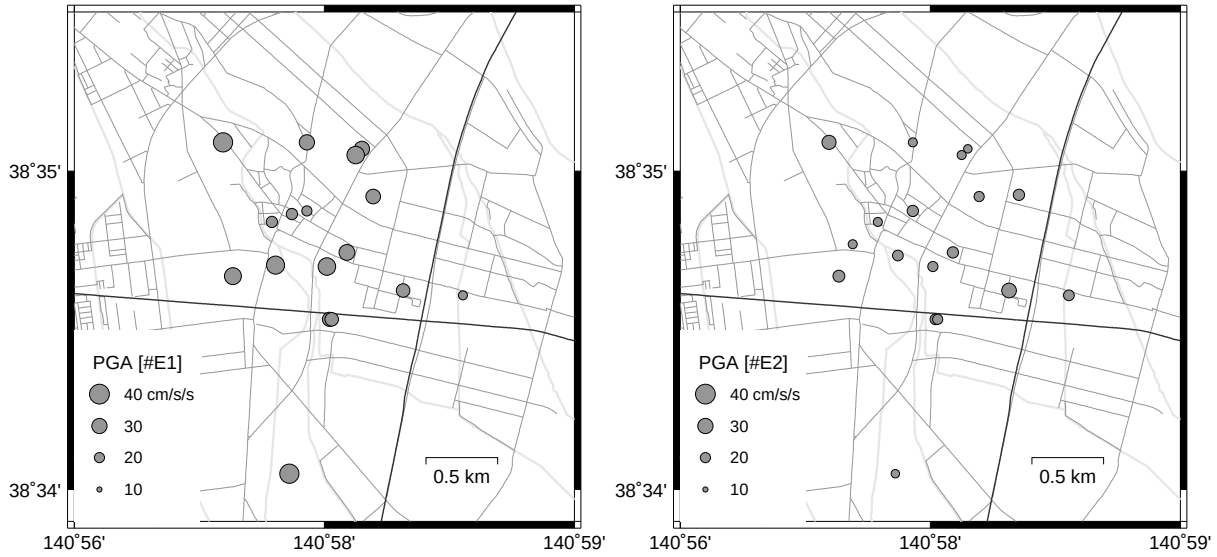

Figure 10: Distribution of peak ground accelerations of the horizontal components of the motions of #E1 recorded on December 10, 2011 (left part), and #E2 recorded on January 1, 2012 (left part): the station locations are presented in Fig.5. (Map data ©OpenStreetMap contributors, CC BY-SA)

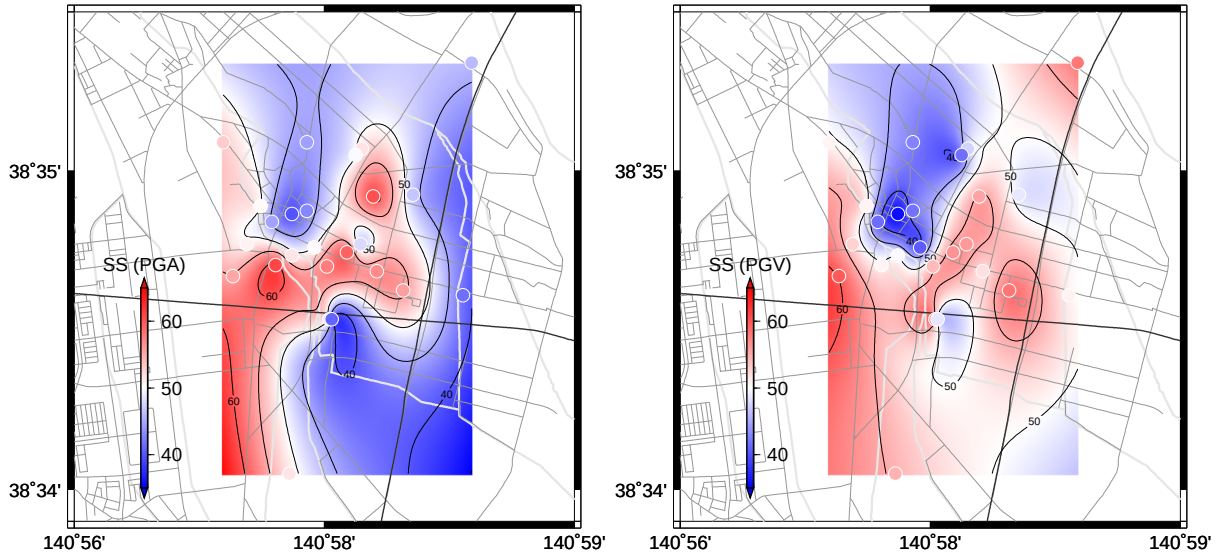

Figure 11: Spatial variation of the PGA and PGV values based on the standard score (SS), presented in Eqs.(1)-(3); the value of 50 reflects the average value. (Map data ©OpenStreetMap contributors, CC BY-SA)

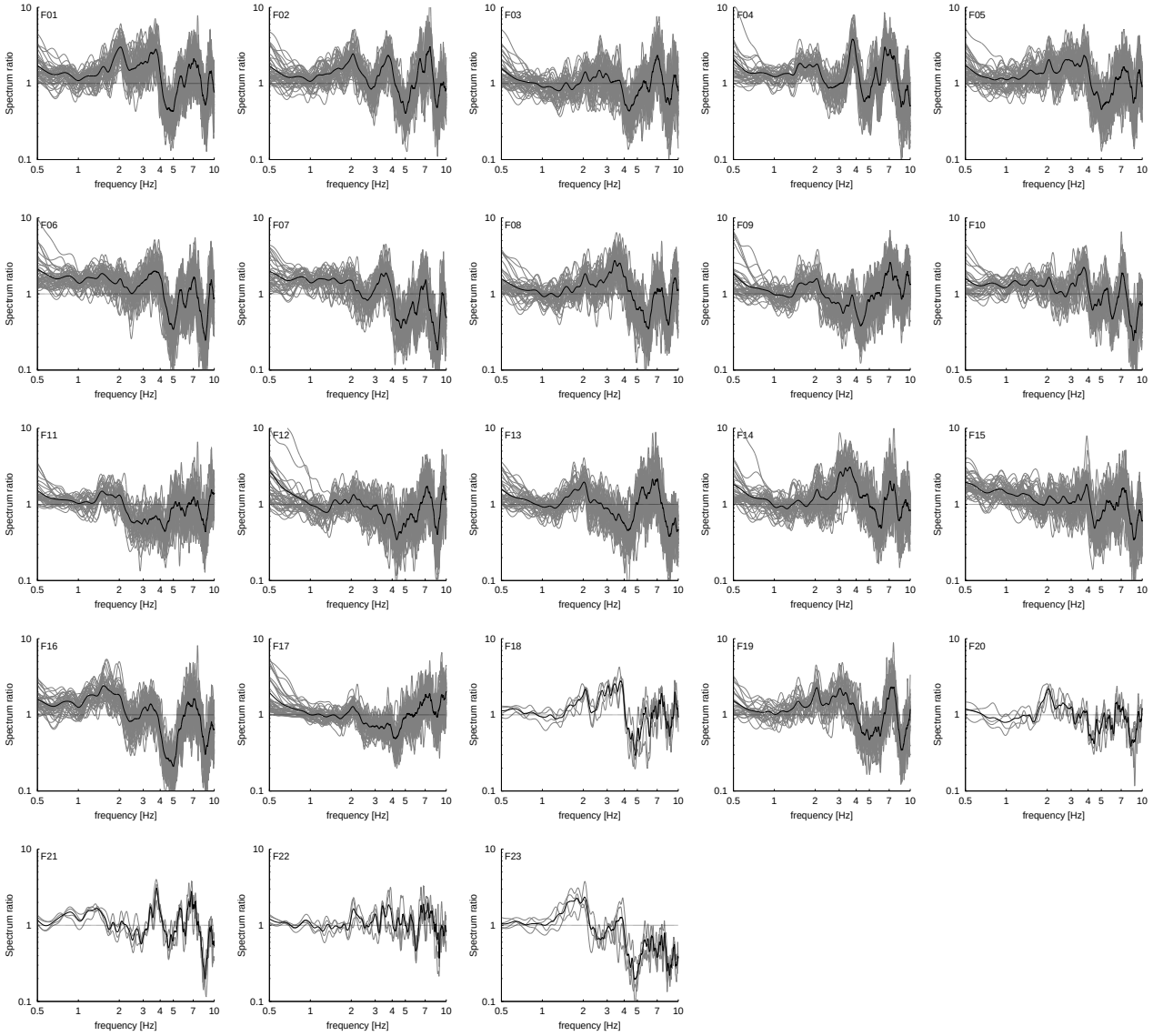

Figure 12: Horizontal spectral ratios of the data at Stations F01-F23 with respect to those at the K-NET MYG006 station during the selected 23 earthquakes. The thick lines indicate the average.